Metallophysics and Advanced Technologies
Металофіз. новітні технол.
Metallofiz. Noveishie Tekhnol.
2026, vol. 48, No. 1, pp. 99–110
https://doi.org/10.15407/mfint.48.01.0099
Reprints available directly from the publisher

PACS numbers: 61.72.Bb, 61.72.jd, 64.70.dm, 66.10.C-, 66.30.-h, 66.30.Fq

Formation of an Amorphous Phase during Quenching of a Metal Melt

A. I. Karasevskii and A. Yu. Naumuk

G. V. Kurdyumov Institute for Metal Physics, N.A.S. of Ukraine,
36 Academician Vernadsky Blvd.,
UA-03142 Kyiv, Ukraine

As demonstrated, variations in the thickness of the molten-metal layer lead to changes in the temperature distribution across the melt and, consequently, in the magnitude of the thermodiffusion force acting on vacancies. The redistribution of vacancies driven by this force results in microstructural reorganization of the melt. At relatively large melt thicknesses, the thermodiffusion force near the surface is insufficient to affect significantly the vacancy distribution, thus, failing to inhibit crystallization processes.

Key words: amorphization, vacancies, temperature gradient, thermodiffusion, phase transition.

Показано, що зміна товщини шару розтопленого металу приводить до змін у розподілі температури по товщині розтопу, а отже, і до зміни величини термодифузійної сили, що діє на вакансії. Перерозподіл вакансій, зумовлений цією силою, спричиняє перебудову мікроструктури розтопу. За відносно великої товщини розтопу термодифузійна сила поблизу поверхні є недостатньою для істотного впливу на розподіл вакансій, а тому не здатна ефективно пригнічувати процеси кристалізації.

Ключові слова: аморфізація, вакансії, ґрадієнт температури, термодифузія, фазовий перехід.

(Received 12 May, 2025; in final version, 11 September, 2025)

Corresponding author: Artem Yuriiovych Naumuk
E-mail: artem.naumuk@gmail.com

Citation: A. I. Karasevskii and A. Yu. Naumuk, Formation of an Amorphous Phase during Quenching of a Metal Melt, *Metallofiz. Noveishie Tekhnol.*, **48**, No. 1: 99–110 (2026), DOI: 10.15407/mfint.48.01.0099

1. INTRODUCTION

In the scientific literature, numerous studies have highlighted the similarity in the evolution of macroscopic properties across different materials during vitrification [1, 2]. Specifically, during the vitrification of metal melts, properties such as specific volume, thermal-expansion coefficients, enthalpy, and elastic moduli exhibit analogous changes. This consistency in properties' evolution suggests a commonality in the vitrification mechanisms of the studied melts. Moreover, the typically high cooling rates required to achieve melt amorphization underscore the dominant role of thermal processes in vitrification.

The most widely employed method for amorphizing metal melts is rapid quenching typically achieved by depositing a thin layer of melt onto the cold surface of a massive metal substrate. In this process, heat is transferred from the melt to the substrate, establishing a temperature gradient within the molten layer. This gradient initiates thermodiffusion processes, particularly, the directed diffusion of mobile melt constituents such as impurity atoms or vacancies [3] (interpreted as holes in the Frenkel's model of liquids [4]). Under suitable conditions, specifically, with an appropriate magnitude and orientation of the temperature gradient, these vacancies migrate toward the free surface of the melt, where they annihilate with surface atoms. This leads to a depletion of free sites near the surface, thereby, suppressing atomic self-diffusion and preventing the nucleation of crystalline phases that would otherwise induce melt crystallization [6]. However, this method for producing amorphous metals presents several significant limitations. Experimental studies [1] have established that only thin melt layers can be successfully amorphized by this approach. For each type of metallic alloy, there exists a critical melt-layer thickness, beyond which amorphization does not occur. The value of this critical thickness depends on the alloy composition and typically ranges from 20 to 400 μm.

In the present work, we demonstrate that variations in the thickness of the molten metal layer lead to changes in the temperature distribution across the melt, and consequently, in the magnitude of the thermodiffusion force acting on vacancies. The redistribution of vacancies, driven by this force, results in microstructural reorganization of the melt. At relatively large melt thicknesses, the thermodiffusion force near the surface is insufficient to affect significantly the vacancy distribution, thus, failing to inhibit crystallization processes.

2. THEORETICAL DETAILS

2.1. Temperature Distribution in the Melt Layer

Let us consider the initial moment of time ($t = 0$), when a layer of mol-

ten metal of thickness l and temperature U_1 is deposited onto the flat surface of a massive metal substrate ($x = 0$) with an initial temperature U_0 ($U_0 >> U_1$) (Fig. 1).

As a result of heat exchange, heat is transferred from the molten layer to the metal substrate, and the temperature distribution within the melt $T(x, t)$ is governed by the standard heat-conduction equation [7]:

$$T_t(x,t) = a^2 T_{xx}(x,t)\,, \tag{1}$$

where $T_t(x, t)$ and $T_{xx}(x, t)$ are the partial derivatives of the temperature distribution with respect to time and spatial coordinate, respectively. Here, $a^2 = k/c\rho$ is the thermal diffusivity, k is the thermal conductivity, c is the specific heat capacity of the melt, and ρ is its density. The solution of Eq. (1) must satisfy the initial condition

$$T(x,0) = U_0 \text{ at } 0 \le x \le l\,, \tag{2}$$

the condition of no heat exchange at the free surface of the melt:

$$T_x(l,t) = 0\,, \tag{3}$$

and the condition of heat exchange according to Newton's law between the melt layer and the metal:

$$T_x(0,t) - h[\,T(0,t) - U_1] = 0\,, \tag{4}$$

where h is the heat-transfer coefficient and U_1 is the temperature of the metal.

The temperature distribution within the melt is obtained from the solution of Eq. (1):

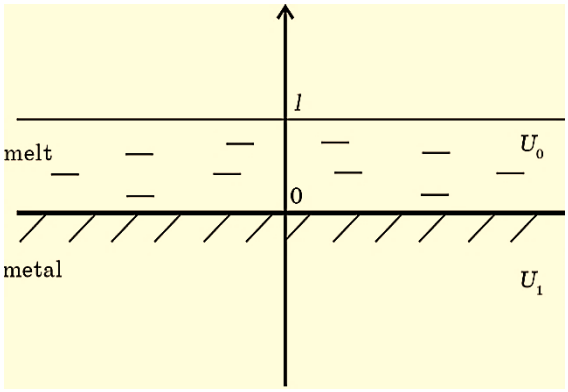

Fig. 1. A layer of molten metal on the flat surface of a metal substrate.

$$T(x,t) = U_1 + 4(U_0 - U_1)\sum_{n=1}^{\infty} \frac{\sin\mu_n}{(\sin 2\mu_n + 2\mu_n)} \cos\mu_n \left(1 - \frac{x}{l}\right) e^{-\frac{t}{\tau_n}}, \qquad (5)$$

where μ_n are eigenvalues of the boundary value problem (1)–(4), the determination of which reduces to solving Eq. (4), which can be written as

$$\frac{\mu_n}{hl} = \operatorname{ctg}\mu_n, \qquad (6)$$

where l is the thickness of the melt layer. Then, the characteristic time of thermal relaxation τ_n in Eq. (5) is given by

$$\tau_n = \left(\frac{l}{a}\right)^2 \frac{1}{\mu_n^2}. \qquad (7)$$

The temperature gradient within the molten-metal layer is given by

$$\frac{\partial T(x,t)}{\partial x} = \frac{4(U_0 - U_1)}{l} \sum_{n=1}^{\infty} \frac{\mu_n \sin\mu_n}{(\sin 2\mu_n + 2\mu_n)} \sin\mu_n \left(1 - \frac{x}{l}\right) e^{-\frac{t}{\tau_n}}, \qquad (8)$$

and depends on the thickness of the molten-metal layer.

In the case of thin melt layers, the temperature gradient within the melt layer is sufficiently large and changes linearly with the thickness of the melt layer (relative thickness of the melt $\kappa = l/l_0$, $hl_0 = 5$, $\kappa \geq 1$; Fig. 2*b*), initiating a constant thermodiffusion effect on the vacancies throughout the entire melt layer. This leads to the majority of vacancies migrating out of the molten-metal layer and a decrease in the number of free sites available for self-diffusion of melt atoms.

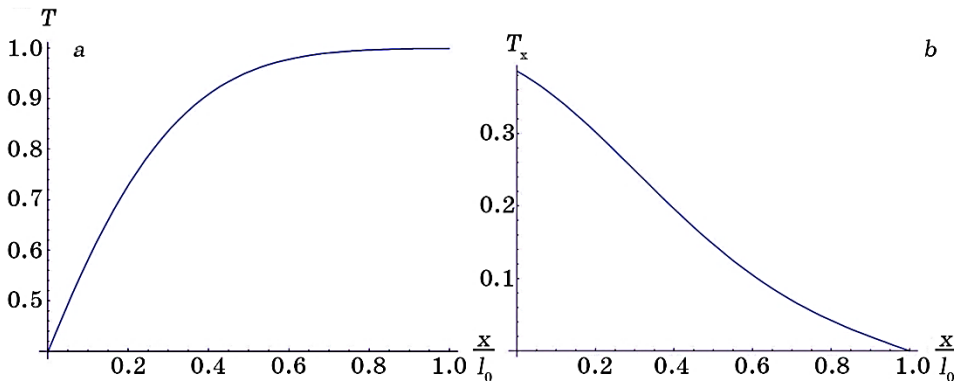

Fig. 2. Co-ordinate dependence of temperature (*a*) and temperature gradient (*b*) in a thin melt layer ($\kappa = 1$, $l = l_0$, $t/\tau_n = 0.1$).

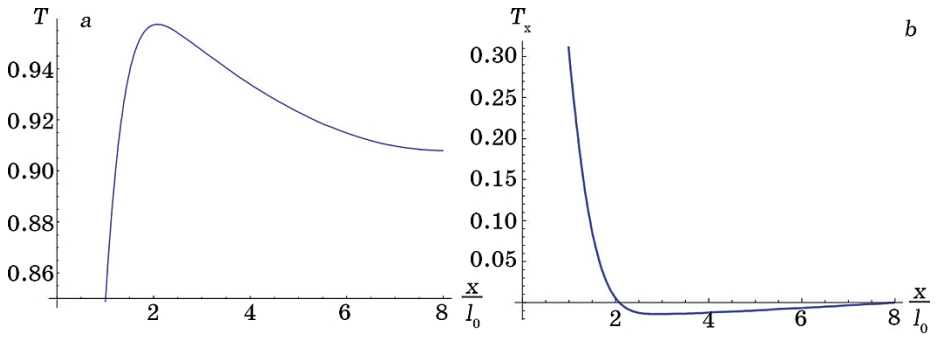

Fig. 3. Co-ordinate dependence of temperature (*a*) and temperature gradient (*b*) in a thick melt layer ($\kappa = 0.125$, $l = 8l_0$, $t/\tau_n = 0.3$).

In an increase in the thickness of the molten-metal layer, it will affect the temperature distribution and temperature gradient within the melt (Fig. 3). In this case, in the sufficiently wide near-surface region of the melt $2l_0 \le x \le 8l_0$ (Fig. 3, *b*), the temperature gradient is small, and the thermodiffusion effect on vacancies is practically absent. That is, for $\kappa < 1$, the melt layer behaves thermodynamically similarly to a massive homogeneous liquid.

The dependence of the temperature gradient on the melt-layer thickness leads to a dimensional dependence of the vacancy distribution within the melt, which is due to the dimensional dependence of the thermodiffusion flux of vacancies $j_{TD}(x, t)$ [3]:

$$j_{TD}(x,t) = -D_v \frac{\partial c(x,t)}{\partial x} + D_T \frac{\partial T(x,t)}{\partial x} c(x,t), \qquad (9)$$

where $c(x, t)$ is the volumetric vacancy density in the melt layer,

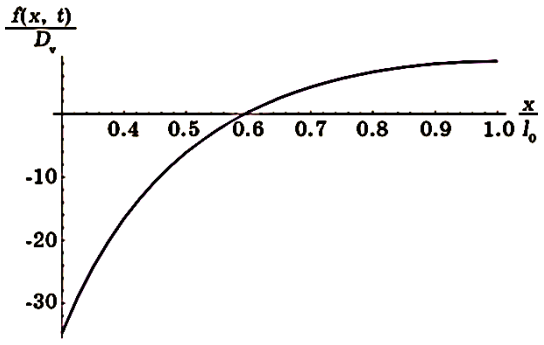

Fig. 4. The distribution of $f(x,t)/D_v$ in the thin melt layer ($\kappa = 1$).

$$D_{\mathrm{v}}(x,t)=\frac{q^2}{\tau_0}e^{-\frac{\upsilon}{k_{\mathrm{B}}T(x,t)}} \tag{10}$$

is the vacancy-diffusion coefficient [3], q is the average interatomic distance in the melt, τ_0 is the average activation time for an atom to transition across the potential barrier to an adjacent vacancy, υ is the height of the potential barrier,

$$D_{\mathrm{T}}(x,t)=D_{\mathrm{v}}\left(\frac{\upsilon}{k_{\mathrm{B}}T(x,t)^2}\right), \tag{11}$$

is the thermodiffusion coefficient of vacancies [3].

The vacancy distribution within the melt layer is governed by the diffusion equation $\frac{\partial c(x,t)}{\partial t}=-\mathrm{div}J_{\mathrm{TD}}(x,t)$, which can be rewritten as

$$\frac{\partial c(x,t)}{\partial t}=D_{\mathrm{v}}(x)\frac{\partial^2 c(x,t)}{\partial x^2}+f(x,t)\,c(x,t), \tag{12}$$

where $f(x, t)$ is the thermodiffusion driving force acting on the vacancies:

$$f(x,t)=-\left(\frac{\upsilon}{k_{\mathrm{B}}TT(x,t)}\right)\left(\frac{\upsilon}{k_{\mathrm{B}}T(x,t)}\frac{T'(x,t)^2}{T(x,t)^2}-2\frac{T'(x,t)^2}{T(x,t)^2}+\frac{T''(x,t)}{T(x,t)}\right). \tag{13}$$

When the melt-layer thickness is increased by 8 times ($\kappa=0.125$), the thermodiffusion driving force of vacancies $f(x, t)$ (13) is shown in Fig. 5.

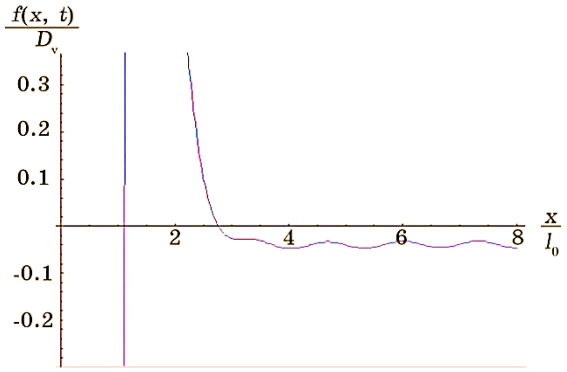

Fig. 5. The distribution of $f(x,t)/D_{\mathrm{v}}$ in the case of a thick melt layer ($\kappa=0.125$).

2.2. The Distribution of Vacancies in the Melt Layer

Let us first consider the escape of defects (vacancies) through the outer boundary ($x = l$) of a molten layer of thickness l, which is located on the surface of the metal, and assume that the temperature of the metal substrate and the melt within the layer are equal, *i.e.*, $f(x, t) = 0$. In this case, the distribution of defects in the layer is governed by the driving force:

$$\frac{\partial c(x,t)}{\partial t} = D_{\mathrm{v}}(x)\frac{\partial^2 c(x,t)}{\partial x^2} + f(x,t)\,c(x,t)\,, \tag{14}$$

where $f(x, t)$ is the driving force, which depends on defect concentration in the layer ($t \geq 0$). We also assume that the boundary of the metal ($x = 0$) is impermeable to defects, *i.e.*,

$$\left.\frac{\partial c}{\partial x}\right|_{x=0} = 0\,. \tag{15}$$

At the surface of the molten layer, vacancies annihilate with surface atoms of the liquid:

$$\left.\frac{\partial c}{\partial x}\right|_{x=l} = -\frac{\beta}{D_{\mathrm{v}}}c(l,t)\,; \tag{16}$$

β is the probability of a vacancy capturing a surface atom.

It is assumed that, at the initial moment $t = 0$, vacancies are uniformly distributed throughout the volume of the melt:

$$c(x,0) = c_0\,. \tag{17}$$

The solution of Eq. (14) can be sought in the form of a Fourier series

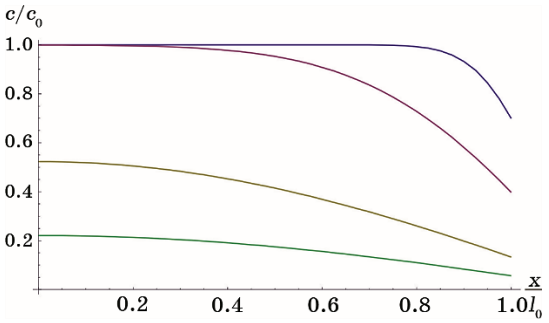

Fig. 6. Change in defect concentration across the thickness of the melt layer during the diffusion-driven escape of defects through the free surface of the molten layer.

expansion [7]:

$$c(x,t) = \sum_{k=1}^{\infty} A_k \cos\left(\mu_k \frac{x}{l}\right) e^{-\frac{t}{\tau_k}}, \tag{18}$$

where

$$\tau_k = \frac{l^2}{D_v} \frac{1}{\mu_k^2}, \tag{19}$$

is the characteristic time of thermal relaxation. Taking into account the orthogonality of the eigenfunctions (16) and (18) gives

$$A_k = \frac{2c_0}{\left(1 + \frac{\sin 2\mu_k}{2\mu_k}\right)} \frac{\sin \mu_k}{\mu_k}, \tag{20}$$

where μ_k are the reduced eigenvalues of Eq. (14), which are determined from the solution of Eq. (16):

$$\operatorname{ctg}\mu_k = \frac{\mu_k}{\beta l}. \tag{21}$$

From Eq. (18), taking into account Eqs. (20) and (21), we obtain:

$$c(x,t) = 2c_0 \sum_{k=1}^{\infty} \frac{1}{\left(1 + \frac{\sin 2\mu_k}{2\mu_k}\right)} \frac{\sin \mu_k}{\mu_k} \cos\left(\mu_k \frac{x}{l}\right) e^{-\frac{t}{\tau_k}}. \tag{22}$$

2.3. Dimensional Effects during Amorphization

As previously shown [6], the preferential escape of vacancies through the surface of the melt reduces the number of available sites for atomic self-diffusion within the melt layer, which leads to the blocking of atomic self-diffusion in the metallic melt and is the cause of the formation of the amorphous state in the molten metal layer.

Since the temperature gradient in the melt layer (8) depends on its thickness (Figs. 2, 3), the magnitude of the thermodiffusion flux (9) and the vacancy distribution within the melt will also depend on the melt layer thickness.

$$\frac{\partial c(x,t)}{\partial t} = D_v(x) \frac{\partial^2 c(x,t)}{\partial x^2} + f(x,t)c(x,t), \tag{23}$$

where $f(x, t)$ is the thermodiffusion force (14) acting on the vacancies.

2.4. Semipermeable Boundary

The thermodiffusion behaviour of the vacancy subsystem of a crystal changes significantly when one of the boundaries of the crystal plate, for example, the upper one, becomes permeable to vacancies.

Let us assume that at the surface ($x = l$) 'annihilation' of bulk vacancies with surface atoms occurs, where the surface atoms are sufficiently numerous and relatively free to move along the crystal surface. This process can be formally described as convective absorption of vacancies by surface atoms.

$$\left.\frac{\partial c}{\partial \eta}\right|_{\eta=1} = -\frac{\beta l}{D_v}\left(c(1,t) - c_0\right), \tag{24}$$

where β is the probability of a vacancy capturing a surface atom. In Eq. (24), it is assumed that the concentration of surface atoms is close to unity.

The lower boundary of the crystal remains impermeable to vacancies:

$$\left.\frac{\partial c}{\partial \eta}\right|_{\eta=0} = 0\,. \tag{25}$$

The distribution of vacancies within the sample volume will be governed by a non-uniform parabolic equation:

$$\frac{\partial c(\eta,t)}{\partial t} = a_0{}^2 \frac{\partial^2 c(\eta,t)}{\partial \eta^2} + F(\eta)c(\eta,t)\,, \tag{26}$$

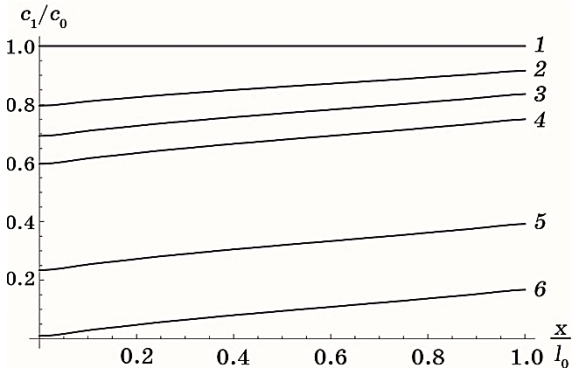

Fig. 7. The vacancy concentration distribution in the melt layer: $D_v = 6\cdot10^{-5}$ cm^2/s, $B = 5$, $\alpha = 0.3$, $a = 3\cdot10^{-8}$ cm, $\beta l/D_v = 1$, $\tau_0 = 10^{-13}$ s. *1*—$t/\tau_0 = 0$; *2*—$t/\tau_0 = 0.3$; *3*—$t/\tau_0 = 0.5$; *4*—$t/\tau_0 = 0.7$; *5*—$t/\tau_0 = 1.5$; *6*—$t/\tau_0 = 2$.

where

$$F(\eta) = a_0{}^2 B_0 \alpha^2 q(\eta) \tag{27}$$

is the thermodiffusion driving force acting on the vacancies.

The solution to the non-uniform parabolic equation (26), which satisfies (24) and (25), can be found in the form of a Fourier series expansion in terms of the eigenfunctions $\cos(\kappa_n \eta)$,

$$c(\eta, t) = \frac{1}{2} A_0(t) + \sum_{n=1}^{\infty} A_n(t) \cos(\kappa_n \eta) e^{-\frac{t}{\tau_{D,n}}}, \tag{28}$$

where $\tau_{D,n} = l^2 \Big/ \left(D_v \kappa_n^2 \right)$.

Let us represent the function $F(\eta)$ and the initial vacancy concentration distribution in the sample $c(\eta, 0)$ also in the form of a Fourier series

$$F(\eta) = \frac{1}{2} F_0 + \sum_{n=1}^{\infty} F_n \cos(\kappa_n \eta), \tag{29}$$

where

$$F_0 = 2a_0{}^2 B_0 \alpha^2 \int_0^1 q(\eta) d\eta, \; F_n = 2a_0{}^2 B_0 \alpha^2 \int_0^1 q(\eta) \cos(\kappa_n \eta) d\eta, \tag{30}$$

κ_k are eigenvalues of Eq. (26), which are determined from the condition (25). Similarly, the initial vacancy distribution

$$c(\eta, 0) = \frac{1}{2} \varphi_0 + \sum_{n=1} \varphi_n \cos(\kappa_n \eta), \tag{31}$$

where

$$\varphi_0 = 2 \int_0^1 c(\eta, 0) d\eta, \; \varphi_k = 2 \int_0^1 c(\eta, 0) \cos(\kappa_k \eta) d\eta. \tag{32}$$

Initially, in the last term of Eq. (26), let us assume $c(\eta, t) = c_0$, which allows obtaining an analytical expression for $c(\eta, t)$ at small $t < t_D$:

$$c_1(\eta, t) = c_0 \left(1 + \left(\frac{1}{2} F_0(t) t + \sum_{n=1}^{\infty} F_n(t) \tau_n \left(1 - e^{-\frac{t}{\tau_n}} \right) \cos(\kappa_n \eta) \right) \right). \tag{33}$$

According to Eq. (26), the thermodiffusion motion of vacancies is determined by the last term in Eq. (26), and the subsequent refinement of the distribution $c(\eta, t)$ will follow from the solution of the following equation

$$\frac{\partial c_2(\eta, t)}{\partial t} = a_0^{\,2} \frac{\partial^2 c_2(\eta, t)}{\partial \eta^2} + F(\eta) c_1(\eta, t), \tag{34}$$

$$c_2(\eta, t) = c_0 + \left(\frac{1}{2} F_0 \int_0^t c_1(\eta, \tau) d\tau + \sum_{n=1}^{\infty} \left[F_n \int_0^t c_1(\eta, \tau) e^{\tau/\tau_n} d\tau \right] e^{t/\tau_n} \cos(\kappa_n \eta) \right). \tag{35}$$

In each specific case, the process of successive approximations can be limited based on the required accuracy of the calculations.

3. CONCLUSIONS

The temperature gradient in a multicomponent medium initiates a thermodiffusion flux of the components of the medium, directed along the temperature gradient. In the case of crystals, one of these components, always present in the solids, are vacancies, which relatively easily diffuse through the crystal, enabling the self-diffusion of its atoms. In this work, an equation is derived to describe the thermodiffusion redistribution of vacancies in the temperature gradient field, and solutions to this equation are found. It is shown that the creation of a temperature gradient in a crystal of finite size leads to a non-uniform vacancy distribution, the degree of non-uniformity of which depends both on the magnitude of the temperature gradient and the boundary conditions of the crystal. If the boundaries of the crystal are blocked, a stationary non-uniform vacancy distribution is established within the crystal, with the vacancy concentration increasing from the cold to the hot region of the crystal [3]. Unblocking the boundary in the hot region of the crystal leads to the outflow of vacancies from the crystal volume (Fig. 6) and with a significant temperature gradient results in the restructuring of the medium's microstructure [12].

It should be noted that thermodiffusion processes could lead to the removal of various types of defects or impurity atoms from the medium's volume, *i.e.*, the creation of a temperature gradient in a multicomponent medium leads to the purification of the medium and the rebuilding of its microstructure [12]. Due to the fact that the creation of a significant temperature gradient is only possible in relatively small regions of the medium or in small-sized crystals, in this work the thermodiffusion of vacancies is considered using the example of a thin crystalline plate with a thickness l, the surfaces of which are at different temperatures.

AUTHORS' CONTRIBUTIONS

A. I. Karasevskii devised the main conceptual ideas, formulated a mathematical model, performed calculations for vacancies distribu-

tion in the melt layer and supervised the findings of this work. A. Yu. Naumuk verified analytical approaches, conducted a literature review, performed calculations for temperature distribution in the melt layer, plotted the graphs, and prepared the manuscript of the paper. All authors approved the final version of the manuscript.

REFERENCES

1. K. Suzuki, X. Fuzimori, and K. Hasimoto, *Amorfnyye Metally* [Amorphous Metals] (Moskva: Metallurgiya: 1987) (Russian translation).
2. T. V. Tropin, J. W. P Schmelzer, and V. L. Aksenov, *Phys.-Usp.*, **59**, No. 1: 42 (2016).
3. A. I. Karasevskii and A.Yu. Naumuk, *Metallofiz. Noveishie Tekhnol.*, **42**, No. 12: 1667 (2020) (in Ukrainian).
4. Ya. I. Frenkel, *Kineticheskaya Teoriya Zhidkostey* [Kinetic Theory of Liquids] (Moskva: Nauka: 1975) (in Russian).
5. P. G. Debenedetti and F. H. Stillinger, *Nature*, **410**: 259 (2001).
6. A. I. Karasevskii and A.Yu. Naumuk, *Metallofiz. Noveishie Tekhnol.*, **41**, No. 9: 1205 (2019) (in Russian).
7. A. N. Tikhonov and A. A. Samarskii, *Equations of Mathematical Physics* (New York: Dover Publications, Inc.: 1990).